SCIENCE CHINA
Information Sciences

• LETTER •

June 2019, Vol. 62 069405:1–069405:3
https://doi.org/10.1007/s11432-018-9659-0

A physical channel-potential and drain-current model for asymmetric dual-gate a-IGZO TFTs

Minxi CAI & Ruohe YAO*

School of Electronic and Information Engineering, South China University of Technology, Guangzhou 510641*, China*

Received 5 July 2018/Revised 23 October 2018/Accepted 7 November 2018/Published online 28 March 2019

Citation Cai M X, Yao R H. A physical channel-potential and drain-current model for asymmetric dual-gate a-IGZO TFTs. Sci China Inf Sci, 2019, 62(6): 069405, https://doi.org/10.1007/s11432-018-9659-0

Dear editor,

A dual-gate (DG) structure demonstrably has improved the device performance and stability of amorphous InGaZnO (a-IGZO) thin-film transistors (TFTs), making circuits faster, less power-consuming, and more stable [1–3]. Physical device modeling has thus generated much interest in circuit design. Ref. [4] derived simple equations describing the DC performance of DG a-IGZO TFTs, empirically based on DG MOSFET models. Ref. [5] proposed an analytical potential model for a-IGZO TFTs with a synchronized symmetric DG (SDG) structure. In previous work, we modeled the threshold voltage and drain current of SDG a-IGZO TFTs by considering the physical properties of active films [6]. There are, nonetheless, several notable challenges. First, perfectly symmetric DG configurations are difficult to fabricate, and also that the two gates are often biased separately. Second, the charge-sheet approximation becomes invalid in DG devices showing bulk accumulation. Moreover, conventional DG MOSFET models do not apply to DG a-IGZO TFTs, where basic semiconductor equations with the sub-gap density of states (DOS) are more difficult to solve.

Given that asymmetric DG (ADG) configurations are more commonly used than SDG, we derived accurate solutions of Poisson's equation and expressions for the physical drain current in ADG a-IGZO TFTs.

Potential model. Band diagrams of the device are shown in Figure 1. Within the gradual channel approximation, Poisson's equation is written $\nabla^2\varphi = -\frac{\mathrm{d}E}{\mathrm{d}x}$. By considering trap-limited conduction (TLC) in a-IGZO, integrating Poisson's equation from 0 to x yields the electric field

$$-E = \frac{\mathrm{d}\varphi}{\mathrm{d}x} = \pm\left\{\alpha + \frac{2q}{\varepsilon_\mathrm{s}}\left[N_\mathrm{t}\varphi_\mathrm{t}\exp\left(\frac{\varphi - V_\mathrm{CH}}{\varphi_\mathrm{t}}\right) + N_\mathrm{f}\varphi_\mathrm{th}\exp\left(\frac{\varphi - V_\mathrm{CH}}{\varphi_\mathrm{th}}\right)\right]\right\}^{1/2}, \quad (1)$$

where φ and V_CH are, respectively, the electrostatic potential and quasi-Fermi potential, ε_s is the permittivity of a-IGZO, $N_\mathrm{f} = N_\mathrm{C}\exp(\frac{-\varphi_\mathrm{F0}}{\varphi_\mathrm{th}})$, $N_\mathrm{t} = N_\mathrm{TA}\frac{\pi T/T_\mathrm{t}}{\sin(\pi T/T_\mathrm{t})}\exp(\frac{-\varphi_\mathrm{F0}}{\varphi_\mathrm{t}})$, φ_F0 is the potential difference between the conduction-band edge and the initial position of the Fermi level, N_C is the effective density of states in the conduction band, N_TA is the total number of trap states per unit volume, $\varphi_\mathrm{th} = \frac{kT}{q}$, $\varphi_\mathrm{t} = \frac{kT_\mathrm{t}}{q}$, T is the room temperature, T_t is the characteristic temperature of trap states, and $\alpha = (\frac{\mathrm{d}\varphi}{\mathrm{d}x})^2|_{x=0} - \frac{2q}{\varepsilon_\mathrm{s}}[N_\mathrm{t}\varphi_\mathrm{t}\exp(\frac{\varphi_\mathrm{B}-V_\mathrm{CH}}{\varphi_\mathrm{t}}) + N_\mathrm{f}\varphi_\mathrm{th}\exp(\frac{\varphi_\mathrm{B}-V_\mathrm{CH}}{\varphi_\mathrm{th}})]$, in which φ_B is the potential at the bottom surface. The other symbols have their usual meanings.

Boundary conditions at the bottom and top surfaces of the active layer can be formulated from Gauss's law as

$$\begin{aligned} -\varepsilon_\mathrm{s}\,(\mathrm{d}\varphi/\mathrm{d}x)|_{x=0} &= C_\mathrm{oxB}(V_\mathrm{GBf} - \varphi_\mathrm{B}), \\ \varepsilon_\mathrm{s}\,(\mathrm{d}\varphi/\mathrm{d}x)|_{x=t_\mathrm{s}} &= C_\mathrm{oxT}(V_\mathrm{GTf} - \varphi_\mathrm{T}), \end{aligned} \quad (2)$$

where $C_\mathrm{oxB(oxT)}$ denotes the bottom-gate (BG) or top-gate (TG) capacitance per unit area,

* Corresponding author (email: phrhyao@scut.edu.cn)

$V_{\mathrm{GBf(GTf)}}$ is the BG or TG bias with the flat-band voltage, φ_{T} is the top-surface potential, and t_{s} is the channel layer thickness.

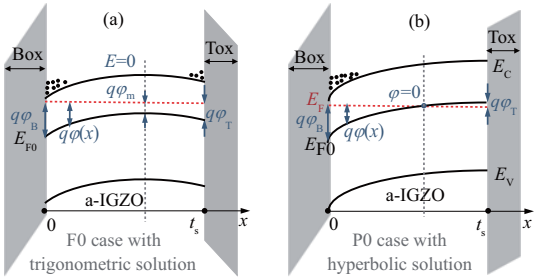

Figure 1 (Color online) Band diagrams in the vertical (x–) direction to the channel for (a) the F0 case and (b) the P0 case.

The integral of (1) cannot be calculated directly. The sub-gap DOS and the occurrence of TLC in a-IGZO suggest that the trapped and free charges dominate conduction for low and high gate voltages, respectively. Thus, an effective characteristic temperature T_{eff}, or its equivalent voltage $\varphi_{\mathrm{eff}}=\frac{kT_{\mathrm{eff}}}{q}$, is introduced. Eq.(1) is rewritten as

$$-E=\frac{\mathrm{d}\varphi}{\mathrm{d}x}=\pm\sqrt{\alpha_{\mathrm{eff}}+(F_{\mathrm{t}}+F_{\mathrm{f}})\exp\left(\frac{\varphi-V_{\mathrm{CH}}}{\varphi_{\mathrm{eff}}}\right)}, \quad (3)$$

where $\alpha_{\mathrm{eff}}=(\frac{C_{\mathrm{oxB}}}{\varepsilon_{\mathrm{s}}})^2(V_{\mathrm{GBf}}-\varphi_{\mathrm{B}})^2-(F_{\mathrm{t}}+F_{\mathrm{f}})\exp(\frac{\varphi_{\mathrm{B}}-V_{\mathrm{CH}}}{\varphi_{\mathrm{eff}}})$, $F_{\mathrm{t}}=\frac{2qN_{\mathrm{t}}\varphi_{\mathrm{t}}}{\varepsilon_{\mathrm{s}}}$, $F_{\mathrm{f}}=\frac{2qN_{\mathrm{f}}\varphi_{\mathrm{th}}}{\varepsilon_{\mathrm{s}}}$. As the gate voltage increases, φ_{eff} gradually changes from being approximately equal to φ_{t} to approaching φ_{th}. Thus, Eq. (3) is equivalent to (1). The method used for obtaining φ_{eff} will be described below. We here focus on solving (3), first by taking $V_{\mathrm{GBf}}>V_{\mathrm{GTf}}$ as an example. By integrating the right-hand side of (3) from 0 to x, we obtain

$$\varphi(x)=V_{\mathrm{CH}}-2\varphi_{\mathrm{eff}}\ln\left\{\sqrt{\frac{F_{\mathrm{t}}+F_{\mathrm{f}}}{(-)-\alpha_{\mathrm{eff}}}}\cdot\sin(\mathrm{h})\left[\frac{\sqrt{(-)-\alpha_{\mathrm{eff}}}}{2\varphi_{\mathrm{eff}}}x+\beta_{\mathrm{eff}}^{(*)}\right]\right\}, \quad (4)$$

where $\beta_{\mathrm{eff}}^{(*)}=\arcsin(\mathrm{h})\left[\sqrt{\frac{(-)-\alpha_{\mathrm{eff}}}{F_{\mathrm{t}}+F_{\mathrm{f}}}}\exp(-\frac{\varphi_{\mathrm{B}}-V_{\mathrm{CH}}}{2\varphi_{\mathrm{eff}}})\right]$. Combining (2) with (4), we obtain an equation for calculating φ_{B}:

$$\frac{C_{\mathrm{oxT}}}{\varepsilon_{\mathrm{s}}}(V_{\mathrm{GTf}}-\varphi_{\mathrm{T}})=-\sqrt{(-)-\alpha_{\mathrm{eff}}}\cdot\cot(\mathrm{h})\left[\frac{\sqrt{(-)-\alpha_{\mathrm{eff}}}}{2\varphi_{\mathrm{eff}}}t_{\mathrm{s}}+\beta_{\mathrm{eff}}^{(*)}\right], \quad (5)$$

where φ_{T} is expressed by (4) at $x=t_{\mathrm{s}}$. The related parentheses in (4) and (5) are ignored when $\alpha_{\mathrm{eff}}<0$, corresponding to the trigonometric solution or the zero-field (F0) case (Figure 1(a)) [7]. These parentheses will be kept if $\alpha_{\mathrm{eff}}>0$, indicating the hyperbolic solution or the zero-potential (P0) case (Figure 1(b)). For devices at given DG biases, the form of the solution must be determined first. By applying $\alpha_{\mathrm{eff}}=0$, we obtain

$$\varphi_{\mathrm{Bcr}}=V_{\mathrm{GBf}}-2\varphi_{\mathrm{eff}}W_0\left[\sqrt{\frac{\varepsilon_s^2(F_{\mathrm{t}}+F_{\mathrm{f}})}{4\varphi_{\mathrm{eff}}^2C_{\mathrm{oxB}}^2}}\cdot\exp\left(\frac{V_{\mathrm{GBf}}-V_{\mathrm{CH}}}{2\varphi_{\mathrm{eff}}}\right)\right], \quad (6)$$

which is the critical bottom-surface potential when the two forms of the solution in (4) and (5) are equivalent, and W_0 is the Lambert W function. Substituting (6) into (5) with α_{eff}=0, we obtain the critical TG voltage as

$$V_{\mathrm{GTfcr}}=V_{\mathrm{CH}}-2\varphi_{\mathrm{eff}}\ln(\Gamma_{\mathrm{Bcr}})-\frac{\varepsilon_{\mathrm{s}}\sqrt{F_{\mathrm{t}}+F_{\mathrm{f}}}}{C_{\mathrm{oxT}}\Gamma_{\mathrm{Bcr}}}, \quad (7)$$

where $\Gamma_{\mathrm{Bcr}}=\frac{t_{\mathrm{s}}\sqrt{F_{\mathrm{t}}+F_{\mathrm{f}}}}{2\varphi_{\mathrm{eff}}}+\exp(-\frac{\varphi_{\mathrm{Bcr}}-V_{\mathrm{CH}}}{2\varphi_{\mathrm{eff}}})$. If $V_{\mathrm{GTf}}>V_{\mathrm{GTfcr}}$, the trigonometric form is chosen, otherwise the hyperbolic form is chosen in (5) to solve for φ_{B}. Once φ_{B} is calculated, potential distributions in the active layer can be obtained accordingly using (4).

By considering the case where either only trapped or free carriers are present in (1) and (2), and applying the same procedure as in (4)–(7), the bottom-surface potential with only the trapped ($\varphi_{\mathrm{B\_t}}$) or free charge ($\varphi_{\mathrm{B\_f}}$) is obtained. These can then be combined as

$$\varphi_{\mathrm{Bcon}}=\frac{\varphi_{\mathrm{B\_t}}}{1+e^{(V_{\mathrm{GBf}}-V_{\mathrm{eq}})}}+\frac{\varphi_{\mathrm{B\_f}}}{1+e^{(V_{\mathrm{eq}}-V_{\mathrm{GBf}})}}, \quad (8)$$

where V_{eq} is the V_{GBf} when $\varphi_{\mathrm{B\_t}}=\varphi_{\mathrm{B\_f}}$. The quantity φ_{eff} can thus be calculated by equating the exponential terms in (1) and (3) with φ_{Bcon}, expressed as

$$\varphi_{\mathrm{eff}}=\Phi(\varphi_{\mathrm{Bcon}})=\left.\frac{\varphi_{\mathrm{Bcon}}}{\ln[F(\varphi_{\mathrm{Bcon}})/(F_{\mathrm{t}}+F_{\mathrm{f}})]}\right|_{V_{\mathrm{CH}}=0}, \quad (9)$$

where $F(\varphi_{\mathrm{Bcon}})=F_{\mathrm{t}}\exp(\frac{\varphi_{\mathrm{Bcon}}}{\varphi_{\mathrm{t}}})+F_{\mathrm{f}}\exp(\frac{\varphi_{\mathrm{Bcon}}}{\varphi_{\mathrm{th}}})$. Note that, if $V_{\mathrm{GTf}}>V_{\mathrm{GBf}}$, the above equations still apply when swapping the subscripts "B" and "T". In the F0 case, the potential extremum (φ_{m}) can be obtained by setting $E=0$ in (3), giving $\varphi_{\mathrm{m}}=V_{\mathrm{CH}}+\varphi_{\mathrm{eff}}\ln(\frac{-\alpha_{\mathrm{eff}}}{F_{\mathrm{t}}+F_{\mathrm{f}}})$.

Drain current model. To derive the drain current, we first consider Pao-Sah's double integral

$$I_{\mathrm{DS}}=\int_0^{V_{\mathrm{DS}}}\int_{\varphi_{\mathrm{B}}}^{\varphi_{\mathrm{T}}}\frac{\mu W}{L}qN_{\mathrm{f}}\exp(\frac{\varphi-V_{\mathrm{CH}}}{\varphi_{\mathrm{th}}})\frac{\mathrm{d}\varphi\mathrm{d}V_{\mathrm{CH}}}{-E}, \quad (10)$$

where μ is the carrier mobility, W and L are the channel width and length, and $V_{\rm DS}$ is the drain-to-source voltage. Following the method of Pierret and Shields [8], the partial derivative of (1) with respect to $V_{\rm CH}$ gives

$$\exp\left(\frac{\varphi-V_{\rm CH}}{\varphi_{\rm th}}\right)=\frac{\varphi_{\rm th}}{F_{\rm f}}\left[\frac{{\rm d}\alpha}{{\rm d}V_{\rm CH}}-\frac{2E\partial E}{\partial V_{\rm CH}}-\frac{F_{\rm t}}{\varphi_{\rm t}}\exp\left(\frac{\varphi-V_{\rm CH}}{\varphi_{\rm t}}\right)\right]. \quad (11)$$

An approximation of the third term in (11) yields

$$\exp\left(\frac{\varphi-V_{\rm CH}}{\varphi_{\rm th}}\right)=\frac{\varphi_{\rm th}}{F_{\rm f}}\left\{\frac{{\rm d}\alpha}{{\rm d}V_{\rm CH}}-\frac{2E\partial E}{\partial V_{\rm CH}}-\frac{1}{\varphi_{\rm t}}\left[\xi\left(F_{\rm t}+F_{\rm f}\right)\exp\left(\frac{\varphi-V_{\rm CH}}{\theta\varphi'_{\rm eff}}\right)-F_{\rm f}\exp\left(\frac{\varphi-V_{\rm CH}}{\varphi_{\rm th}}\right)\right]\right\}, \quad (12)$$

where $\varphi'_{\rm eff}=\Phi(\varphi_{\rm B})$, ξ and θ are fitting parameters. With this approach and after some mathematical manipulations (see Appendix A), the drain current becomes

$$I_{\rm DS}=\delta A\left\{t_{\rm s}\left[\left(\alpha_{\rm L}-\alpha_0\right)-B\left(\alpha'_{\rm effL}-\alpha'_{\rm eff0}\right)\right]+D\left[\frac{C_{\rm oxB}}{\varepsilon_{\rm s}}\left(\varphi_{\rm BL}-\varphi_{\rm B0}\right)\left(2V_{\rm GBf}-\varphi_{\rm BL}-\varphi_{\rm B0}\right)+\frac{C_{\rm oxT}}{\varepsilon_{\rm s}}\left(\varphi_{\rm TL}-\varphi_{\rm T0}\right)\left(2V_{\rm GTf}-\varphi_{\rm TL}-\varphi_{\rm T0}\right)+2\left(K_{\rm L}-K_0\right)\right]\right\}, \quad (13)$$

where $A=\frac{\mu W}{L}\frac{qN_{\rm f}\varphi_{\rm t}\varphi_{\rm th}}{F_{\rm f}(\varphi_{\rm t}-\varphi_{\rm th})}$, $B=\frac{\xi\theta\varphi'_{\rm eff}}{\varphi_{\rm t}}$, $D=1-B$, $\alpha_{\rm L(0)}$ is the value of α corresponding to $V_{\rm CH}=V_{\rm DS}$ ($V_{\rm CH}=0$), $\varphi_{\rm BL(B0)}$ and $\varphi_{\rm TL(T0)}$ are the values of $\varphi_{\rm B}$ and $\varphi_{\rm T}$ for $V_{\rm CH}=V_{\rm DS}$ ($V_{\rm CH}=0$). Note that the function δ avoids singularities once $B\geqslant 1$ in the deep subthreshold region. The quantities $\alpha'_{\rm effL(eff0)}$ and $K_{\rm L(0)}$ are intermediate variables, expressed as shown in Appendix A.

Model validation and discussion. The potential model was verified by rigorous numerical calculations, as presented in Appendix B. The verification of the proposed drain-current model is given in Appendix C, in which the transfer and output curves are well described under various DG biases. Because of the repulsion and attraction of carriers by the TG field, the transfer curve and threshold voltage show parallel shifts along the BG-voltage axis by a TG-dependent amount. This constitutes an advantage for ADG a-IGZO TFTs with TG control, stemming from the absence of a hole-accumulation layer in a-IGZO. The drain currents and potential distributions for various active-layer thicknesses have also proven to be well characterized by this model. A higher on-state current and a steeper subthreshold slope are observed when the a-IGZO layer is thinner than the Debye length, indicating the extension of the accumulation/depletion layer throughout the a-IGZO bulk. Since no charge-sheet approximation is involved, this model applies also to devices exhibiting bulk accumulation or depletion.

Conclusion. We presented a convergent and efficient solution for the channel potential of ADG a-IGZO TFTs. An expression for the analytical and continuous drain current was then derived, providing a physical interpretation of device DC characteristics. This model provides an effective approach for reducing the complexity induced by the sub-gap DOS, while capturing the basic underlying physics. It can therefore serve as the basis for potential-based models, amenable to implementation in device and circuit simulators.

Acknowledgements This work was supported by National Natural Science Foundation of China (Grant No. 61274085), and Science and Technology Planning Project of Guangdong Province (Grant No. 2015B090909001).

Supporting information Appendixes A–C. The supporting information is available online at info.scichina.com and link.springer.com. The supporting materials are published as submitted, without typesetting or editing. The responsibility for scientific accuracy and content remains entirely with the authors.

References

1 Kim D S, Kwon O K. A small-area and low-power scan driver using a coplanar a-IGZO thin-film transistor with a dual-gate for liquid crystal displays. IEEE Electron Device Lett, 2017, 38: 195–198
2 Jeon C H, Um J G, Mativenga M, et al. Fast threshold voltage compensation AMOLED pixel circuit using secondary gate effect of dual gate a-IGZO TFTs. IEEE Electron Device Lett, 2016, 37: 1450–1453
3 Baek G, Abe K, Kuo A, et al. Electrical properties and stability of dual-gate coplanar homojunction DC sputtered amorphous indium-gallium-zinc-oxide thin-film transistors and its application to AM-OLEDs. IEEE Trans Electron Device, 2011, 58: 4344–4353
4 Baek G, Kanicki J. Modeling of current-voltage characteristics for double-gate a-IGZO TFTs and its application to AMLCDs. J Soc Inf Display, 2012, 20: 237–244
5 Qin T, Huang S X, Liao C W, et al. Analytical channel potential model of amorphous InGaZnO thin-film transistors with synchronized symmetric dual-gate (in Chinese). Acta Phys Sin, 2017, 66: 097101
6 Cai M X, Yao R H. A threshold voltage and drain current model for symmetric dual-gate amorphous InGaZnO thin film transistors. Sci China Inf Sci, 2018, 61: 022401
7 Shi X J, Wong M. Analytical solutions to the one-dimensional oxide-silicon-oxide system. IEEE Trans Electron Device, 2003, 50: 1793–1800
8 Pierret R F, Shields J A. Simplified long-channel MOSFET theory. Solid-State Electron, 1983, 26: 143–147